

## Molecular-dynamics study on atomistic structures of liquid silicon

Manabu Ishimaru, Kou Yoshida, Takashi Kumamoto, and Teruaki Motooka

*Department of Materials Science and Engineering, Kyushu University, Hakozaki, Fukuoka 812-81, Japan*

(Received 27 February 1996)

Structural characteristics of liquid silicon (*l*-Si) have been examined by molecular-dynamics calculations using the Tersoff empirical potential. Generated *l*-Si possesses a broad distribution of the coordination number dominated by the sixfold coordination. The average bond length increases with the coordination number. The bond angle distribution function indicated that *l*-Si has a preference for the bond angles of 60° and 90°. The 60° peak mainly occurs from the atoms with longer bonds of the coordination number  $\geq 5$ . We have also discussed a possible short-range order in *l*-Si that includes the atomic configurations with a close-packed layer, such as the simple hexagonal structure. [S0163-1829(96)05132-6]

### I. INTRODUCTION

It is known that the physical properties of liquid silicon (*l*-Si) show anomalous behavior near the melting temperature  $T_m$  (1414 °C).<sup>1,2</sup> Recently, Kimura and co-workers have accurately measured the density,<sup>3,4</sup> surface tension,<sup>5</sup> and viscosity of *l*-Si as a function of temperature in the range of  $\sim 100^\circ\text{C}$  above  $T_m$ . They have found that there exists a kink in the density, viscosity, and surface tension versus temperature curves at  $\approx 1430^\circ\text{C}$ , and proposed that this is due to a structural change in *l*-Si. Understanding this anomalous behavior is technologically important because the anomalous range is involved in the crystal growth from melted Si such as in the Czochralski method. Therefore, the determination of the microscopic structure of *l*-Si is of great importance, and various models for the short-range order of the liquid phase have been proposed.<sup>6-9</sup> However, to our knowledge, the detailed analysis of the anomalous behavior has not yet been performed.

Molecular-dynamics (MD) simulations provide a useful technique to analyze melting and atomistic structure of the liquid phase. For MD simulations, several empirical interatomic potentials for Si have been proposed by many investigators.<sup>10</sup> We have recently performed MD simulations using the Tersoff potential<sup>11,12</sup> in order to investigate the validity of this potential for *l*-Si.<sup>13</sup> Our simulations have indicated that the static properties of the generated *l*-Si network are in good agreement with those obtained by x-ray-diffraction experiments<sup>6</sup> and *ab initio* MD simulations,<sup>14,15</sup> though the Tersoff potential overestimates greatly the melting temperature. The result suggests that this potential is very useful for the structural analysis of *l*-Si.

In the present study, we carried out MD simulations using the Tersoff potential in order to clarify the local structure of *l*-Si. The results obtained here were compared with those of previous experimental and theoretical researches.

### II. COMPUTATIONAL METHODS

The same computational procedure as that described previously<sup>13</sup> was employed in the present study. MD calculations under constant NVT conditions (where V denotes volume and T denotes temperature) were performed for

$N=512$  atoms in a cubic box with periodic boundary conditions. The density of the MD cell was fixed at 2.33 and 2.57 g/cm<sup>3</sup> for crystalline Si (*c*-Si) and *l*-Si, respectively. We used the Tersoff interatomic potential whose parameters are described in Ref. 12. The forces acting on all particles are analytically calculated by taking the derivative of the potential energy with respect to each atomic position. The Newtonian equations of motion were integrated using a velocity-Verlet algorithm<sup>16</sup> with a time step  $\Delta t=2\times 10^{-3}$  ps. The MD simulations were carried out for  $30\,000\Delta t$  (60 ps), and the system was found to reach equilibrium during this period as judged by the total energies.

### III. RESULTS AND DISCUSSION

Figure 1 shows the potential energies of *c*-Si and *l*-Si generated by the Tersoff potential. The potential energy increases with temperature, and the solid-to-liquid phase transition occurs at about 2750 K for the present time scale (60 ps). This  $T_m$  is slightly higher than that reported by Cook and Clancy ( $2547\pm 22$  K for 140 ps).<sup>17</sup> The calculated value of the latent heat is 45.4 kJ/mol, which is close to the experimental value of 50.6 kJ/mol.<sup>18</sup> Since our MD simulations were performed under a fixed volume, the specific heat at

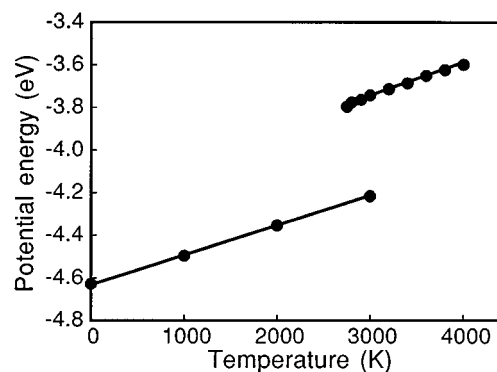


FIG. 1. Configurational energy per atom of Si generated by the Tersoff potential. The hysteresis around 2800 K is due to the difference of simulated densities between crystal and liquid phases. The energy jump at 2750 K corresponds to typical first-order phase transition, and the value of the latent heat is 45.4 kJ/mol.

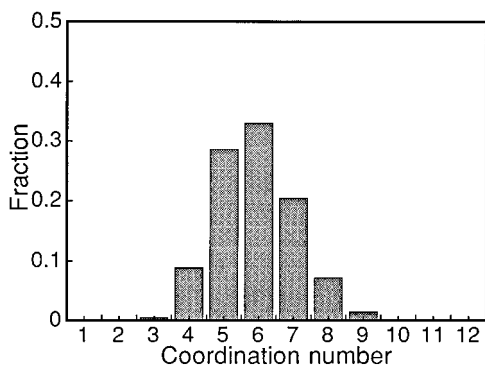


FIG. 2. Distribution of local coordination number in *l*-Si obtained near melting temperature. The simulated temperature is 3000 K. The coordination shell is obtained by counting the number of atoms at a distance shorter than 3.1 Å.

constant volume  $C_v$  can be calculated from the slope of the total energy curves obtained by adding the kinetic energies to the potential energies shown in Fig. 1. For the crystalline and liquid phases,  $C_v$  is equal to 0.92 and 1.02 J/gK, respectively. These values are in good agreement with the specific heat at constant pressure  $C_p$  obtained experimentally.<sup>18</sup> (In condensed matters, the difference between  $C_v$  and  $C_p$  is small.)

The distribution of the number of nearest-neighbor atoms in *l*-Si is shown in Fig. 2. Molten metals usually tend to take a close-packed structure; accordingly the higher coordinations ( $\sim 12$ ) appear. In the case of *l*-Si, however, the sixfold coordination is dominant, and this is consistent with the experimental result that the average coordination number is 6.4.<sup>6</sup> In other words, *l*-Si is rather loosely packed. This indicates the presence of a covalent bonding nature even in the liquid state, though the electronic properties of *l*-Si are metallic.

Typical examples of the local atomic configurations with various (4–9) coordinations in *l*-Si are demonstrated in Fig. 3. One can see that the *l*-Si network consists of various bond lengths that largely deviate from the *c*-Si bond length, 2.35 Å. Figure 4 indicates the average bond length as a function of the coordination number. We can confirm that the average bond length tends to become longer with increase of the coordination number. The similar tendency in the bond length has been also pointed out by Kim and Lee.<sup>19</sup>

Bond angle distributions provide valuable information on the local structural units and their connectivity in the liquid. Figures 5(a) and 5(b) illustrate the bond angle distribution functions  $g(\theta)$  with the cutoff distances of 2.49 and 3.1 Å, respectively. The former corresponds to the covalent cutoff defined by Stich, Car, and Parrinello,<sup>14</sup> and for this cutoff distance the coordination number is 2.2 and the bond angles broadly distribute around the tetrahedral angle (109.5°) [Fig. 5(a)]. On the other hand, for the latter cutoff distance there are two peaks around 60° and 90° in Fig. 5(b) and the 60° peak can be attributed to the atoms with longer bond length as discussed below. This 60° peak increases slightly with the temperature. The results of bond angle distributions as a function of the cutoff distance are in good agreement with

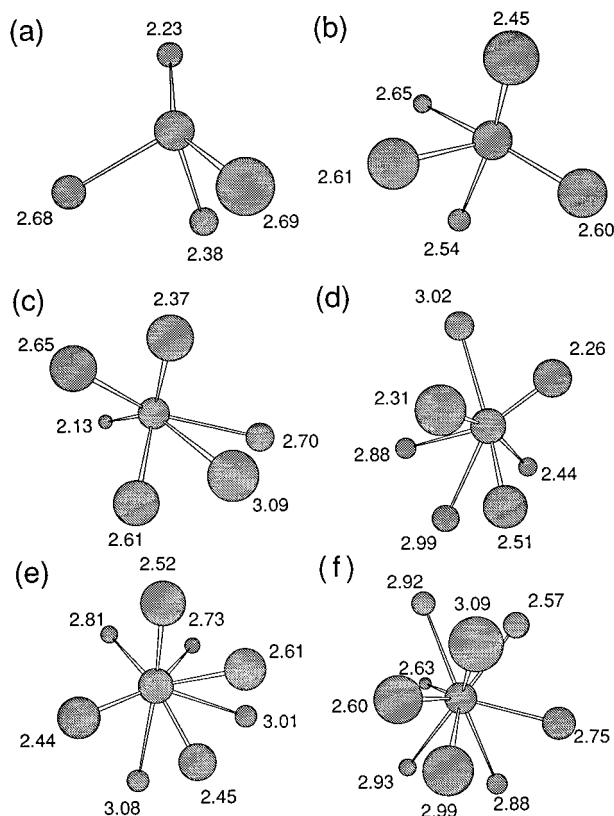


FIG. 3. Typical local structures around atoms with various coordination numbers. The coordination numbers are (a) 4, (b) 5, (c) 6, (d) 7, (e) 8, and (f) 9. Bonds are defined by neighbors within 3.1 Å. The units of bond lengths are in Å. The feature of atomic configuration, e.g., bond length is similar to that reported by Kim and Lee (Ref. 19).

those obtained by *ab initio* calculations<sup>14</sup> and tight-binding MD simulations.<sup>19</sup>

Figure 6 shows the bond angle distribution  $g(\theta)$  of atoms with various coordination numbers. The cutoff distance is set at 3.1 Å. For the fourfold coordination, the bond angles are broadly distributed around the tetrahedral angle, suggesting

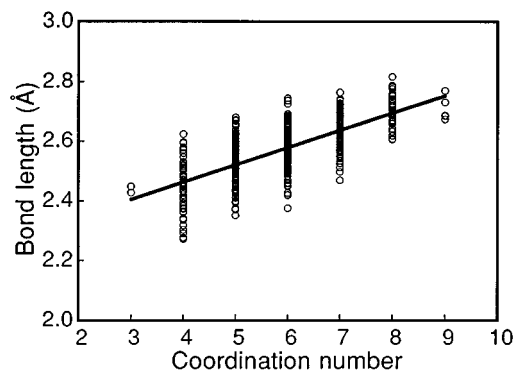


FIG. 4. Average bond length as a function of coordination number. The points are obtained from an atomic configuration of *l*-Si at the end of the simulation period, and the line is obtained from a mean of the least squares. The bond length tends to become long with the increase of the coordination number.

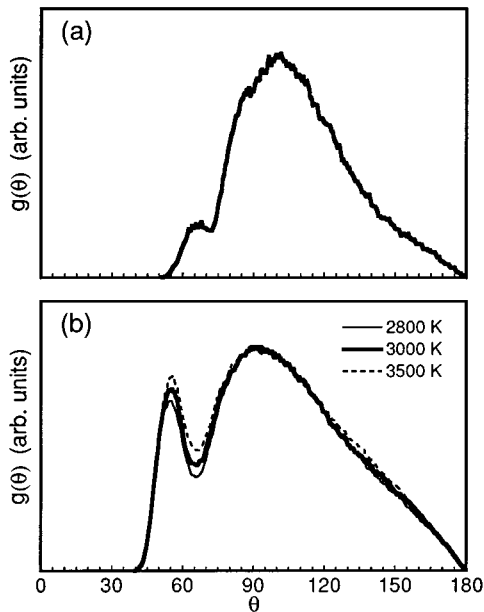


FIG. 5. Bond angle distribution functions of atomic configuration in *l*-Si. The cutoff distance is equal to (a) 2.49 and (b) 3.1 Å, and each distribution is an average over 500 configurations during  $500\Delta t$  (1 ps). The maximum of  $g(\theta)$  exists around the tetrahedral angle in (a), while two peaks of  $60^\circ$  and  $90^\circ$  appear in (b).

the existence of the atomic clusters constructed by  $sp^3$  bonding even in the liquid state. On the contrary, reverse Monte Carlo simulations<sup>9</sup> have shown the presence of an additional peak at  $\theta=60^\circ$  for the fourfold coordination atoms. This

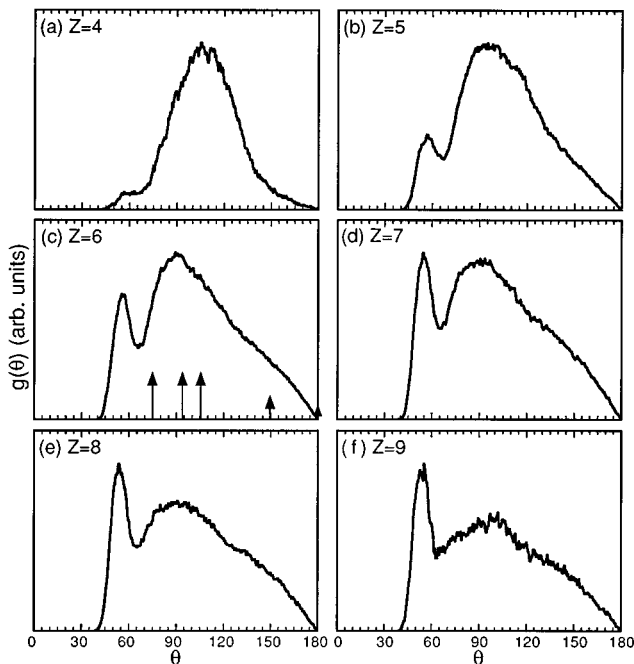


FIG. 6. Partial bond angle distributions for atoms with various coordination numbers. The coordination numbers are (a) 4, (b) 5, (c) 6, (d) 7, (e) 8, and (f) 9. Vertical arrows in (c) correspond to the bond angles between the first six neighboring atoms of  $\beta$ -Sn structure, and the height indicates the quantity. Note that  $60^\circ$  peak mainly occurs from the atomic bondings with over 5 coordination number.

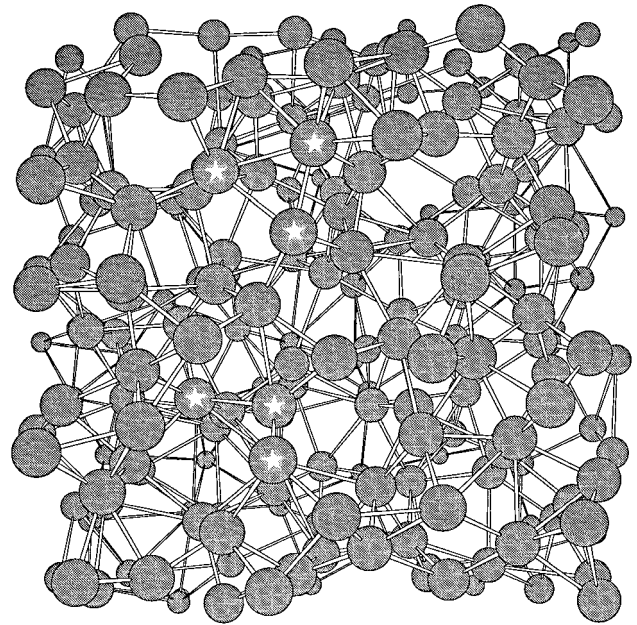


FIG. 7. Snapshot of the *l*-Si network generated by the Tersoff potential. Bonds are defined by neighbors within 3.1 Å. This picture includes 216 particles. Some of the triangular configurations of atoms are indicated by stars.

result disagrees with our result of Fig. 6(a). The discrepancy is attributed to the difference of cutoff distance. That is, the cutoff distance for the reverse Monte Carlo approach (3.26 Å) is longer than that for our simulation.

In the case of the fivefold coordination [Fig. 6(b)], the maximum peak of  $g(\theta)$  shifts toward  $90^\circ$ , and a new peak appears around  $60^\circ$ . This  $60^\circ$  peak becomes prominent as the coordination number increases. That is, the  $60^\circ$  peak seen in Fig. 5(b) is primarily due to the atoms with the coordination numbers more than 5. It is surprising that this peak position does not depend on the coordination numbers. For the short-range order in *l*-Si and *l*-Ge, various structure models have been proposed.<sup>6-9</sup> Some investigators have proposed the existence of the white-tin ( $\beta$ -Sn) structure<sup>8,9</sup> in order to reproduce the shoulder of the first peak in the static structure factor.<sup>6</sup> The  $\beta$ -Sn structure is composed of the four nearest neighbors and two next nearest neighbors, and the bond angles associated with these six neighboring atoms are  $\theta=74.6^\circ, 94.0^\circ, 105.4^\circ, 149.3^\circ,$  and  $180^\circ$ . However, these distributions are not consistent with the  $g(\theta)$  of Fig. 6(c). Many triangular configurations of atoms are actually observed in our simulated *l*-Si (Fig. 7). Therefore, the local structure of *l*-Si cannot be described by the simple  $\beta$ -Sn structure.

As described in Sec. I, anomalous behavior of physical properties has been found in *l*-Si at  $\approx 1430^\circ\text{C}$ .<sup>1-5</sup> This suggests that some structural transformation occurs even in the liquid phase. The short-range ordered structure of *l*-Si must possess the bond angle of  $\approx 60^\circ$ , and show the electronic properties similar to metals. A possible structure model is the simple hexagonal (SH) structure, which is one of the polymorphs in *c*-Si.<sup>20,21</sup> This structure is characterized by simple stacking of the close-packed layer, which is expressed by  $AAA\cdots$  in a similar way to  $ABAB\cdots$  in hcp and

$ABCABC\dots$  in fcc, and its electron density of state is free-electron-like.<sup>22</sup> Koyama and Suzuki<sup>23</sup> have reported that structural transformation between SH and  $\beta$ -Sn can be achieved by simple atomic displacements along the  $[\bar{1}210]$  direction of the SH lattice as illustrated in Fig. 9 of Ref. 23. Thus, we believe that  $l$ -Si includes not only  $\beta$ -Sn but also SH structures and the atomic arrangements fluctuate between these structures.

Recently, Waseda *et al.*<sup>24</sup> have measured the static structure factors of  $l$ -Si at 1440, 1460, and 1520 °C. A characteristic shoulder on the high-wave-number side of the first peak has been found to become slightly obscure as the temperature increases. This suggests that the fraction of the  $\beta$ -Sn type configurations decreases at the higher temperatures, because the shoulder of the first peak can be attributed to the  $\beta$ -Sn structure as mentioned above. Our result that the 60° peak increases with the temperatures [Fig. 5(b)] is consistent with this experimental behavior. The structural fluctuations between SH and  $\beta$ -Sn may cause anomalous behavior of  $l$ -Si near  $T_m$ . More extensive study is currently under way.

#### IV. CONCLUSIONS

The structural properties of  $l$ -Si have been investigated by using MD simulations. The findings of this investigation are as follows:

(1) The  $l$ -Si generated by the Tersoff empirical interatomic potential has atoms with various coordination num-

bers. The distribution is almost symmetric around the sixfold coordination.

(2) The bond length in  $l$ -Si largely deviates from that of  $c$ -Si (2.35 Å), and various bond lengths exist in the  $l$ -Si network. The average bond length tends to become longer with the increase of the coordination number.

(3) The bond angles associated with shorter bonds broadly distribute around the tetrahedral angle, while the bond angles associated with longer bonds peak around 60° and 90°.

(4) The fourfold coordinated atoms have a broad bond angle distribution around the tetrahedral angle. On the other hand, 60° and 90° peaks appear in the atoms with larger coordination numbers. For the local configurations around the atoms with the coordination numbers more than 5, the peak position of  $g(\theta)$  does not depend on the coordination number.

(5) The  $l$ -Si network may consist of not only the  $\beta$ -Sn structural units but also configurations with the close-packed layer such as the SH structure. We believe that structural fluctuations between the  $\beta$ -Sn and SH structure can be attributed to anomalous behavior of physical properties in  $l$ -Si near  $T_m$ .

#### ACKNOWLEDGMENTS

This work was partly supported by the New Energy and Industrial Technology Development Organization through the Japan Space Utilization Promotion Center.

- 
- <sup>1</sup>V. M. Glazov, *Liquid Semiconductors* (Plenum, New York, 1969).
- <sup>2</sup>K. Kakimoto, M. Eguchi, H. Watanabe, and T. Hibiya, *J. Cryst. Growth* **94**, 412 (1989).
- <sup>3</sup>H. Sasaki, E. Tokizaki, K. Terashima, and S. Kimura, *Jpn. J. Appl. Phys.* **33**, 3803 (1994); **33**, 6078 (1994).
- <sup>4</sup>S. Kawanishi, H. Sasaki, S. Takeda, K. Terashima, and S. Kimura, *Jpn. J. Appl. Phys.* **34**, 482 (1995).
- <sup>5</sup>H. Sasaki, Y. Anzai, X. Huang, K. Terashima, and S. Kimura, *Jpn. J. Appl. Phys.* **34**, 414 (1995).
- <sup>6</sup>Y. Waseda and K. Suzuki, *Z. Phys. B* **20**, 339 (1975).
- <sup>7</sup>B. R. Orton, *Z. Naturforsch. A* **30**, 1500 (1975).
- <sup>8</sup>J. P. Gaspard, P. Lambin, C. Mouttet, and J. P. Vigneron, *Philos. Mag. B* **50**, 103 (1984).
- <sup>9</sup>V. Petkov and G. Yunchov, *J. Phys. Condens. Matter* **6**, 10 885 (1994).
- <sup>10</sup>For example, see H. Balamane, T. Halicioglu, and W. A. Tiller, *Phys. Rev. B* **46**, 2250 (1992), and references therein.
- <sup>11</sup>J. Tersoff, *Phys. Rev. B* **38**, 9902 (1988).
- <sup>12</sup>J. Tersoff, *Phys. Rev. B* **39**, 5566 (1989).
- <sup>13</sup>M. Ishimaru, K. Yoshida, and T. Motooka, *Phys. Rev. B* **53**, 7176 (1996).
- <sup>14</sup>I. Štich, R. Car, and M. Parrinello, *Phys. Rev. B* **44**, 4262 (1991).
- <sup>15</sup>J. R. Chelikowsky, N. Troullier, and N. Binggeli, *Phys. Rev. B* **49**, 114 (1994).
- <sup>16</sup>K. Binder and D. W. Heerman, *Monte Carlo Simulation in Statistical Physics, An Introduction* (Springer, Berlin, 1988).
- <sup>17</sup>S. J. Cook and P. Clancy, *Phys. Rev. B* **47**, 7686 (1993).
- <sup>18</sup>J. Q. Broughton and X. P. Li, *Phys. Rev. B* **35**, 9120 (1987).
- <sup>19</sup>E. Kim and Y. H. Lee, *Phys. Rev. B* **49**, 1743 (1994).
- <sup>20</sup>J. Z. Hu and I. L. Spain, *Solid State Commun.* **51**, 263 (1984).
- <sup>21</sup>H. Olijnyk, S. K. Sikka, and W. B. Holzapfel, *Phys. Lett.* **103A**, 137 (1984).
- <sup>22</sup>W. Jank and J. Hafner, *Phys. Rev. B* **41**, 1497 (1990).
- <sup>23</sup>Y. Koyama and H. Suzuki, *Acta Metall.* **37**, 597 (1989).
- <sup>24</sup>Y. Waseda, K. Shinoda, K. Sugiyama, S. Takeda, K. Terashima, and J. M. Toguri, *Jpn. J. Appl. Phys.* **34**, 4124 (1995).